LBL-21920

Lawrence Berkeley Laboratory

UNIVERSITY OF CALIFORNIA

Physics Division

Presented at the XXIII International Conference on High Energy Physics, Berkeley, CA, July 16-23, 1986

COMPARISON OF $q\bar{q}g$ AND $q\bar{q}\gamma$ EVENTS IN e^+e^- ANNIHILATION AT PEP

LBL--21920

DE87 000119

W. Hofmann

July 1986

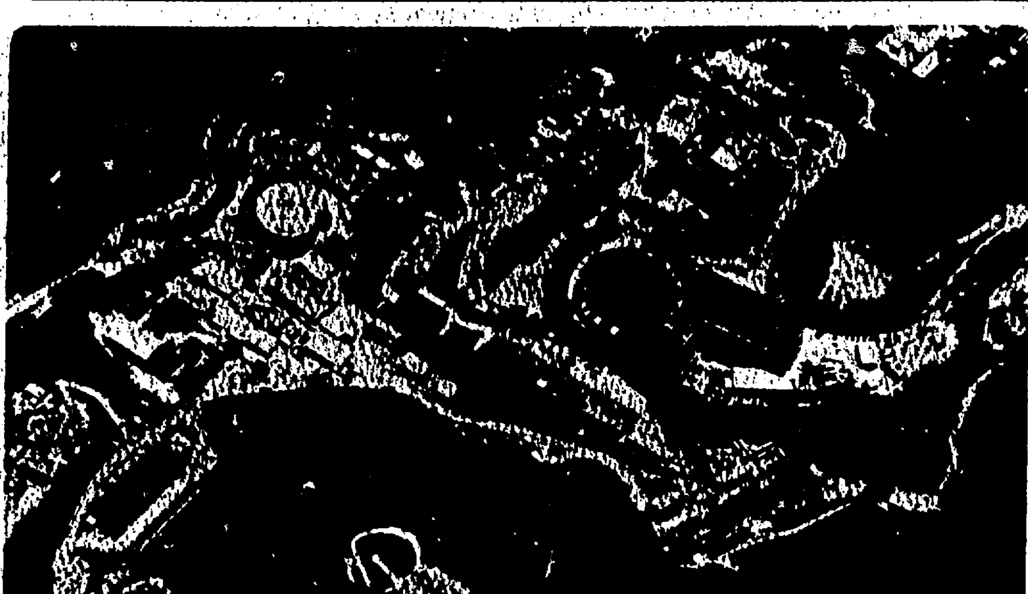

Prepared for the U.S. Department of Energy under Contract DE-AC03-76SF00098

MASTER

LBL-21920

Comparison of $q\bar{q}g$ and $q\bar{q}\gamma$ Events in e^+e^- Annihilation at PEP

Werner Hofmann

Lawrence Berkeley Laboratory

University of California, Berkeley, CA 94720

Presented at the XXIII International Conference on High Energy Physics, 16-23 July 1986, Berkeley, CA

Abstract: In comparing the particle flow in the event plane of three-jet ($q\bar{q}g$) events and of radiative annihilation events ($q\bar{q}\gamma$) for similar kinematic configurations, two PEP experiments find a significant decrease in particle density in the angular region opposite to the gluon jet in $q\bar{q}g$ events, relative to the particle density in the region opposite to the photon in $q\bar{q}\gamma$ events. The effect is predicted both by QCD and by phenomenological string models.

In this paper I will present results from two experiments at PEP, the MARK II and TPC/Two-Gamma, on the comparison of three-jet ($q\bar{q}g$) and radiative annihilation ($q\bar{q}\gamma$) events produced in e^+e^- interactions at 29 GeV. This work was in part motivated by recent QCD predictions[1] concerning the azimuthal distribution of soft gluons in the event plane of events with a large-angle gluon jet. The flow of soft gluons in such events is represented as a coherent sum of bremsstrahlung-like radiation from quark, antiquark, and hard gluon. The calculations predict a particular effect in three-jet events (see fig. 1): in the azimuthal region between q and $\bar{q}$, opposite to the gluon jet, negative interference of radiation from q and $\bar{q}$ and of radiation from the gluon results in a sizable reduction of the soft-gluon density. The effect can be tested directly by comparing ($q\bar{q}g$) three-jet events with events where the gluon is replaced by a radiative photon ($q\bar{q}\gamma$), with otherwise identical kinematics. In the latter events, the negative interference is missing, resulting in a higher particle density in the region between q and $\bar{q}$. The experimental search for this effect tests two different aspects of the theoretical model: the underlying QCD arguments and, since in the experiment hadrons are measured instead of soft gluons, the implicit assumption of local parton-hadron duality (which assumes that the angular distribution hadrons reflects the flow of soft gluons).

The selection of the relevant event samples follows similar principles in both experiments (Fig. 2): planar three-jet $q\bar{q}g$ events are selected using fairly standard jet-finding algorithms (Fig. 2(a)). For $q\bar{q}\gamma$ events, two jets and a coplanar, well-isolated large-angle photon detected in the calorimeter are required (Fig. 2(b)). Since the rate of such events is rather low, the TPC group has considered another type of radiative annihilation event: frequently, the radiative photon is emitted along the beam direction and escapes undetected. However, detection of two non-collinear high energy jets coplanar with the beam line provides a sufficiently clear signature to select such events (Fig. 2(c)). Beyond the general criteria above, both experiments use other detector-specific cuts to enhance purity and quality of the event samples. Details are given in refs. 2,3.

Jet (or photon) energies $E_1 > E_2 > E_3$ are reconstructed from the measured angles between jets. The third (lowest-energy) jet in three-jet events is assumed to be the gluon. Correspondingly, the photon in $q\bar{q}\gamma$ events has to have less energy than either of the two jets. Typical energies are around 13 GeV for jet 1, 10 GeV for jet 2 and 6 GeV for jet 3 or photon. The resulting samples consist of 2537 and 6585 $q\bar{q}g$ candidates for MARK II and TPC, respectively, of 117 and 320 $q\bar{q}\gamma$ candidates and of 1564 TPC events with a photon emitted along the beam line (denoted by $q\bar{q}[\gamma]$). The larger MARK II samples reflect the higher integrated luminosity (215 pb^{-1} as compared to 144 pb^{-1} for the TPC), the slightly higher efficiency for photon detection and less stringent cuts in the jet finding algorithms. Typical sample purities (i.e. the probability that the lowest energy jet/photon is really a gluon or radiative photon) range from 60 to 65% for $q\bar{q}g$ and from 75 to 85% for $q\bar{q}\gamma$, and are about 70% for $q\bar{q}[\gamma]$. Both experiments have performed numerous checks to ensure the integrity of their event samples. For example, in $q\bar{q}\gamma$ events the photon energy is actually measured, and one can compare the measured value with the energy derived from the angles; Fig. 3 shows this comparison for the MARK II data. The $q\bar{q}\gamma$ and $q\bar{q}[\gamma]$ event rates allow a measurement of the electromagnetic coupling constant α, providing an excellent cross-check. The TPC finds ratios of actual to expected event numbers of 0.99 ± 0.14 and 0.98 ± 0.06 for the two samples.

Results are given in Figs. 4 and 5. Fig. 4 shows the particle flow as a function of the angle ϕ in the event plane for the TPC (a) and MARK II data (b). The highest energy jet (1) defines ϕ = 0, jet 2 is typically around 150^o and jet 3 around 230^o. In the angular regions near the cores of jets 1 and 2, the distributions for $q\bar{q}g$ and $q\bar{q}\gamma$ events agree very well. Of course, the third jet is missing in the $q\bar{q}\gamma$ sample. In the region between jets 1 and 2, opposite to gluon jet or photon, both the TPC and MARK II data show a depletion in particle production for $q\bar{q}g$ as compared to $q\bar{q}\gamma$. In order to make this statement quantitative, and to account for the small differences in opening angle between jets 1 and 2 for the different samples, particle distributions are given as a function of the normalized angle $x = \phi/\phi_{12}$ (ϕ_{12} is the angle between jet 1 and jet 2). The direction of jet 1 corresponds to x=0, the jet 2 direction to x=1. Fig. 5 shows the ratio of the particle density per event, $(1/N_{event})(dn/dx)$, for $q\bar{q}g$ and $q\bar{q}\gamma$ events as a function of x. The TPC $q\bar{q}\gamma$ and $q\bar{q}[\gamma]$ data sets and the MARK II $q\bar{q}\gamma$ data set are consistent with each other and shown a clear depletion in particle density opposite to the gluon jet in $q\bar{q}g$ events, as compared to $q\bar{q}\gamma$. Data are consistent with QCD predictions (shaded area in Fig. 5(a)). Based on Monte Carlo simulations using independent-fragmentation schemes (where coherence effects do not occur), both experimental groups have verified that the observed depletion cannot be caused by a bias introduced in event selection or data analysis.

Fig. 4(b) also includes curves based on the Lund string model[4]. The model predicts a depletion effect very similar to the QCD interference effect, and describes the data well. In the string picture, the explanation for the effect is obvious: in $q\bar{q}g$ events, a color string is spanned from the q via the gluon to the $\bar{q}$. The qg and $\bar{q}g$ string segments are moving away from the region between jet 1 and 2. This boost causes a depletion of particle density in the region. This is the well-known "string effect"[5]. In contrast, in $q\bar{q}\gamma$ events the string is spanned directly between q and $\bar{q}$, i.e. between jet 1 and jet 2. At first, the agreement of predictions from string phenomenology and QCD may seem a striking coincidence. An explanation is given in ref. 1: it can be shown that the particle flow predicted in the string model, i.e. the incoherent superposition of particles from the qg and $\bar{q}g$ string segments, reproduces the QCD result up to non-leading terms suppressed by powers of $1/N_c$ (N_c is the number of colors). In other words, string phenomenology can be seen as a neat way to summarize the leading QCD coherence effects. The importance of this result - the equivalence of string model and QCD and the agreement with experiment - is that for the first time we have an indication from QCD why the string model is so eminently successful in the description of event topologies.

This work was supported by the US Department of Energy under contract number DE-AC03-76SF00098. The author acknowledges an A.P. Sloan Fellowship.

References

1 Ya. I. Azimov, Yu. L. Dokshitzer, V.A. Khoze, S.I. Troyan: Phys. Lett. 165B, 147 (1985)

2 H. Aihara et al.: LBL-21543 (1986)

3 P.D. Sheldon et al.: LBL-21872 (1986)

4 B. Andersson, G. Gustafson, G. Ingelman, T. Sjöstrand: Phys. Rep. 97, 33 (1983)

5 W. Bartel et al.: Z. Phys. C21, 37 (1983); Phys. Lett. 134B, 275 (1984); 157B, 340 (1985); H. Aihara et al.: Z. Phys. C28, 31 (1985); M. Althoff et al.: Z. Phys. C29, 29 (1985)

Figure captions

Fig. 1 Directivity diagram of soft gluon flow in $q\bar{q}g$ (solid) and $q\bar{q}\gamma$ (dashed) events, projected into event planes defined by the q and $\bar{q}$ momentum vectors. The distance from the origin represents the density of soft gluons emitted at an angle ϕ with respect to the quark jet. Note that the radial scale is logarithmic. From ref. 1.

Fig. 2 Signatures for the different event types: (a) $q\bar{q}g$, (b) $q\bar{q}\gamma$ (both viewed along the beam axis) and (c) $q\bar{q}[\gamma]$ (viewed from the side)

Fig. 3 Difference between measured and calculated photon energies for MARK II $q\bar{q}\gamma$ events. Δ_γ is defined as $(E_\gamma^{meas.} - E_\gamma^{calc.\ from\ angles})/E_{beam}$. The full line shows the expected distribution in Δ_γ, based on a Monte-Carlo simulation including detector effects.

Fig. 4 Charged track density as a function of the event plane angle ϕ. The distributions are normalized to the number of events in each sample. (a) TPC data, represented in a polar plot corresponding to Fig. 1. (b) MARK II data, for all tracks (top) and for tracks with at least 0.3 GeV/c momentum out of the event plane (bottom). Also shown: predictions of string model ("Lund") and independent-fragmentation model ("Ali").

Fig. 5 Ratio R of the particle flow in $q\bar{q}g$ and $q\bar{q}\gamma$ events, in the region between jets 1 and 2, as a function of the scaled angle $x = \phi/\phi_{12}$. (a) TPC data for the $q\bar{q}\gamma$ and $q\bar{q}[\gamma]$ topologies. The shaded area represents the range of QCD predictions. (b) MARK II data.

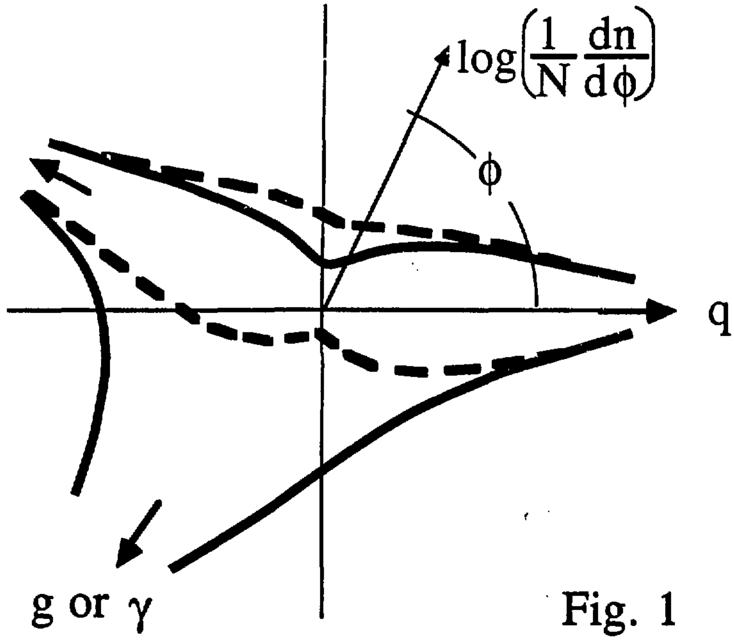

Fig. 1

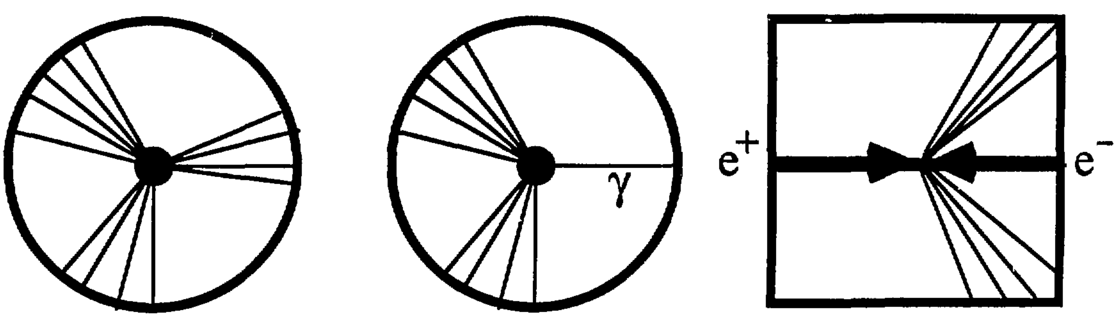

Fig. 2(a) 2(b) 2(c)

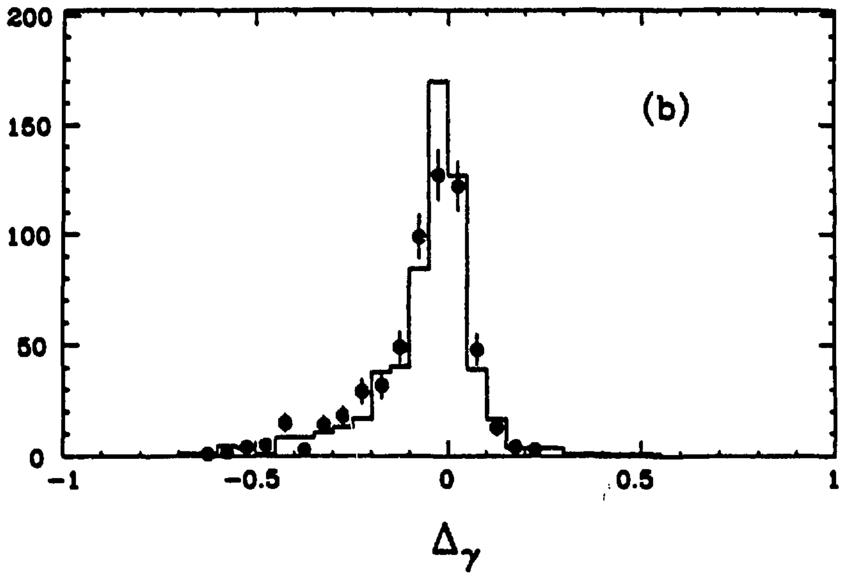

Fig. 3

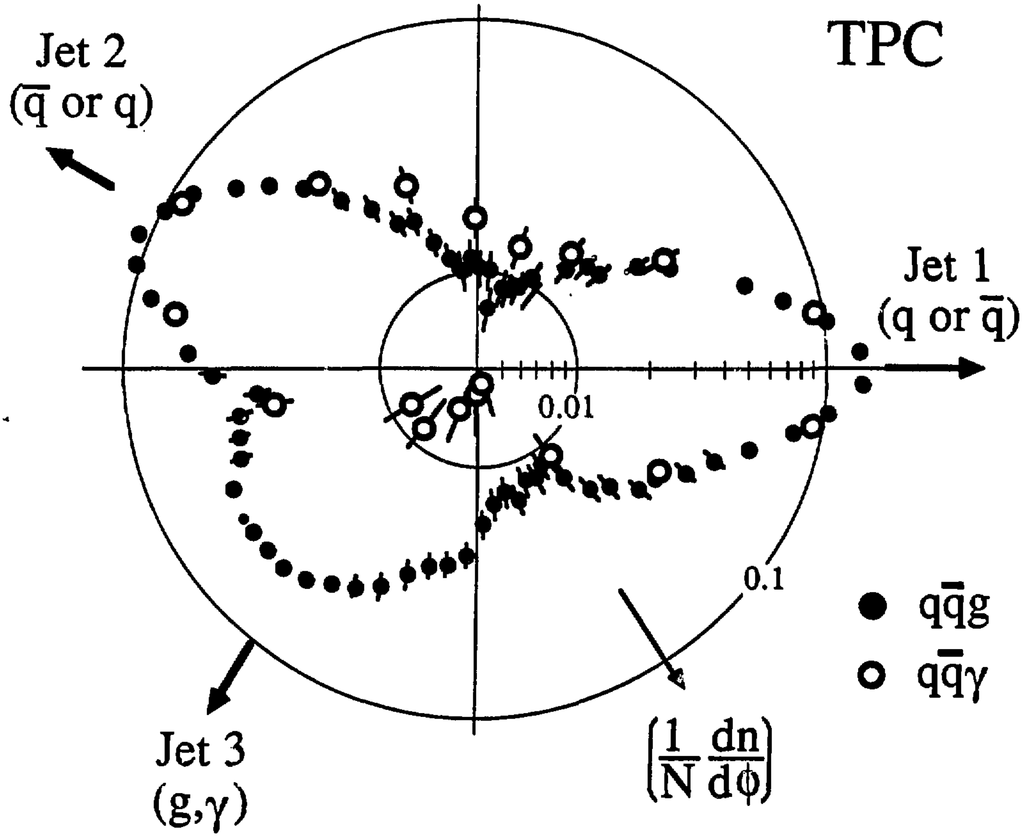

TPC
Jet 2
($\bar{q}$ or q)
Jet 1
(q or $\bar{q}$)
0.01
0.1
Jet 3
(g,γ)
$\left(\frac{1}{N}\frac{dn}{d\phi}\right)$
$q\bar{q}g$
$q\bar{q}\gamma$

Fig. 4(a)

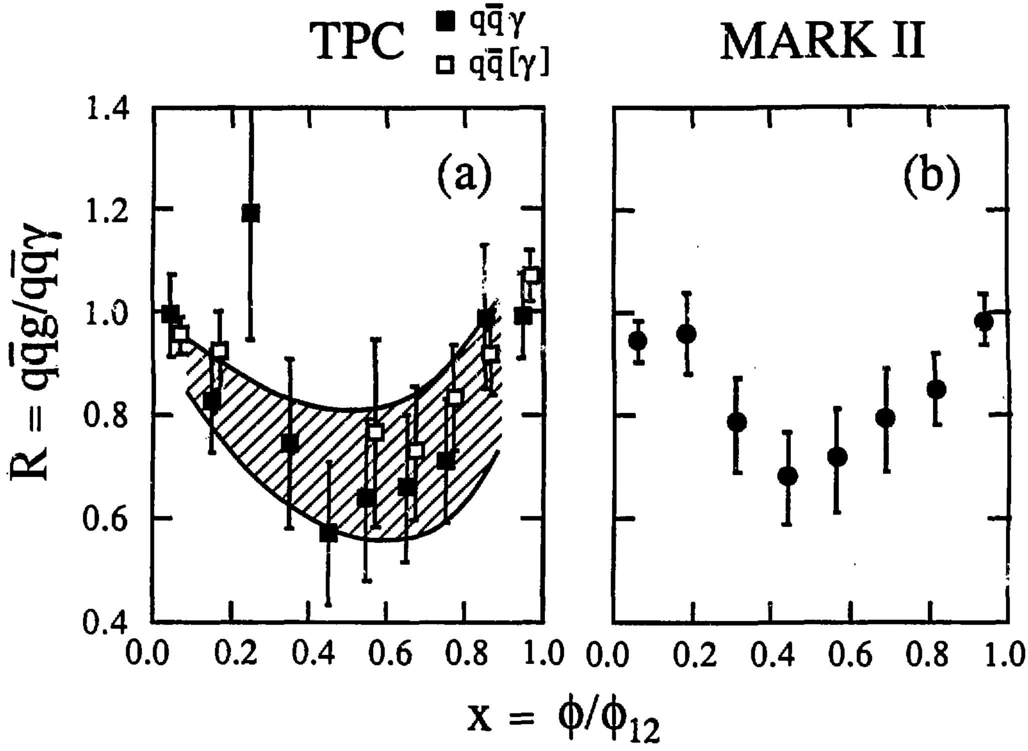
TPC
■ $q\bar{q}\gamma$
□ $q\bar{q}[\gamma]$
MARK II
1.4
1.2
1.0
0.8
0.6
0.4
(a)
(b)
$R = q\bar{q}g/q\bar{q}\gamma$
0.0
0.2
0.4
0.6
0.8
1.0
$x = \phi/\phi_{12}$

Fig. 5